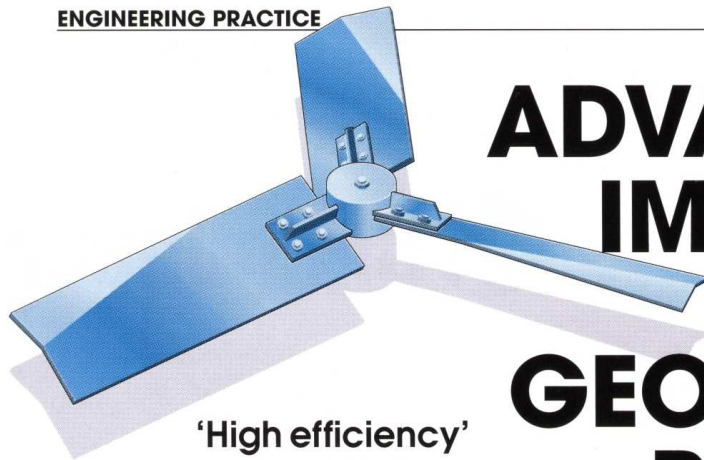


Fasano J.B., Bakker A., Penney W.R. (1994) Advanced Impeller Geometry Boosts Liquid Agitation. Chemical Engineering, August 1994, 7 pages.

## ENGINEERING PRACTICE



**'High efficiency' units outperform their pitched-blade counterparts in blending and heat transfer**

# ADVANCED IMPELLER

# GEOMETRY BOOSTS LIQUID AGITATION

Julian B. Fasano and André Bakker  
Chemineer Inc.  
W. Roy Penney  
University of Arkansas

A traditional agitator impeller often functions as a rather inefficient pump because of the way it produces fluid motion and pressure head. However, one can improve the amount of flow or shear generated by an impeller at constant power consumption and torque by changing its design.

For example, a high-efficiency, axial-flow impeller produces more fluid motion per unit of power at constant torque than an otherwise similar pitched-blade turbine. The more-vigorous fluid motion cuts blend time and enhances heat-transfer in various flow-controlled mixing operations, such as blending of miscible fluids.

For most applications, a higher degree of agitation intensity can be achieved on the same machine by substituting a high-efficiency impeller (Figure 1) for a conventional pitched-blade unit. The high-efficiency impeller

**FIGURE 1 (top of page).** Featuring a larger geometric pitch at the hub than at the tip, a high-efficiency impeller enhances liquid mixing and heat transfer

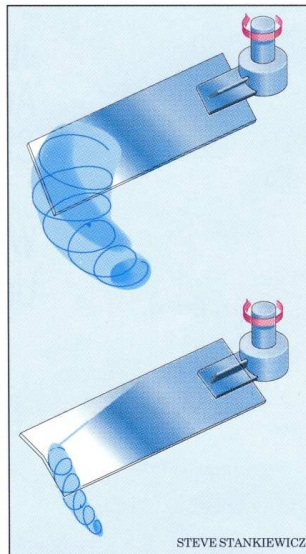


**FIGURE 2.** The larger blade-tip vortex in a four-bladed pitched turbine (other blades not shown above) accounts for its lower efficiency, compared with a three-bladed high-efficiency impeller

features a larger geometric pitch angle (30–60 deg) at the hub than at the tip (10–30 deg). Results from recently conducted controlled experiments indicate the beneficial effects of the high-efficiency impeller on blend time and heat-transfer coefficients in liquid-liquid mixing as well as solids suspension. This article focuses on liquid agitation, with discussions of solids suspension set aside for a forthcoming piece in this series of articles on mixing [1–2].

### Selecting an impeller style

A proper understanding of flow, head and the effect of blade-tip vortices is important in selecting an impeller type for a particular application. Any device that moves fluid can produce some combination of head and flow for a given amount of power:

$$P = \frac{g\rho Q_p H}{\epsilon} \quad (1)$$

The power not used in generating head or flow is dissipated through shear or turbulent eddies. However, this "dissipation" of energy is not necessarily harmful because there are applications where the generation of such

turbulent eddies or vortices is highly desirable. For example, turbulent vortices play an important role during contacting of gases and liquids, mixing of immiscible liquids, and drawing-down of floating solids.

Much of the energy loss from an impeller in turbulent flows is in the form of a blade-tip vortex. Nearly half of the backside of a pitched impeller blade is enveloped with this energy-dissipating vortex, compared with only a small fraction of the backside of a high-efficiency impeller blade (Figure 2). The smaller vortex on the high-efficiency blade accounts for lesser dissipation of energy, and greater production of head or flow instead.

An impeller produces laminar flow when the impeller's Reynolds number ( $N_{Re} = \rho ND^2/\mu$ ) is less than 1. In laminar flow, no vortices are formed from blade tips, even for the pitched-blade turbine, so the performance of the pitched-blade impeller is similar to that of its high-efficiency counterpart. Transitional flow for most impellers is considered to exist between  $N_{Re}$  values of 1 and 10,000. For  $N_{Re} > 10,000$ , the flow is fully turbulent. Recommended impeller styles for transitional and turbulent flows are listed in Table 1.



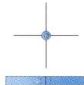

Selection of the correct impeller style is very important as is the number of impellers to be used. That's because an impeller, even a high-efficiency type, cannot provide adequate mixing action beyond a certain liquid level. This maximum liquid level is a function of Reynolds number. Generally, for different ranges of  $N_{Re}$ , the ratio of liquid level to tank diameter ( $Z/T$ ) is used in deciding whether to use single- or dual-impeller agitators (Table 2).

#### Estimate power requirements

Agitator vendors can typically supply the user with the experimentally determined power number ( $N_p$ ), which is a function of impeller type, geometry and  $N_{Re}$ . This power number for four-bladed pitched impeller and three-bladed high-efficiency impeller (designated HE-3) can be obtained from Figure 3. The impeller power requirement can be calculated [3] from:

$$P = N_p \rho N^3 D^5 \quad (2)$$

This equation can also be rearranged

Applications of Impellers		
Impeller style	Preferred $N_{Re}$ range	Recommended applications
Three-bladed, high-efficiency 	$\geq 100$	<ul style="list-style-type: none"> <li>Blending of miscible liquids</li> <li>Solids suspension</li> <li>Heat transfer</li> </ul>
Four-bladed, 45-deg pitched 	$\geq 10$	<ul style="list-style-type: none"> <li>Draw-down of surface solids or gas</li> <li>Coarse immiscible liquid-liquid and gas-liquid dispersions</li> </ul>
Four-bladed, flat 	$\geq 1$	<ul style="list-style-type: none"> <li>Local mixing at tank bottom</li> <li>Transitional- to low-<math>N_{Re}</math> mixing (for <math>1 \leq N_{Re} \leq 500</math>)</li> <li>Agitation during vessel pump-out</li> </ul>
Six-bladed, disc 	$\geq 1$	<ul style="list-style-type: none"> <li>Intense gas-liquid mixing</li> <li>Fine dispersion of immiscible liquids</li> <li>Fast semi-batch reactions</li> </ul>

**TABLE 1.** A number of factors, including the prevalent flow regime, come into play in deciding the right impeller style

to determine impeller diameter when it is desired to load an agitator impeller to a given power level. The torque delivered to the fluid by a single impeller can be computed from the impeller speed and power draw as follows:

$$\tau = \frac{P}{2\pi N} = \frac{N_p \rho N^2 D^5}{2\pi} \quad (3)$$

#### Quantifying agitation intensity

Prior to a pioneering attempt to quantify agitation intensities by Hicks and his coworkers [4], it was customary to broadly rate the degree of agitation intensity in a mixing vessel as "mild," "medium" or "violent." No quantitative technique was available to consistently define these agitation intensities, and therefore, there was no way to insure that such intensities could be replicated on other batch sizes or for other types of mixing applications.

Hicks [4] introduced a relative measure for assessing agitation intensity in pitched-blade impellers by use of a "scale of agitation." Symbolized by  $S_A$  here, this scale of agitation is based on

a characteristic velocity,  $v^*$ , which is determined as follows:

$$v^* = \frac{Q_p}{A_v} \quad (4)$$

$Q_p$  is determined from the pumping number,  $N_q$ , in Figure 4. Ranging from 1 to 10,  $S_A$  is a linear function of the characteristic velocity. Accordingly, a  $S_A$  value of 1 represents a low level, and 10 a high level of agitation intensity.  $S_A$  is readily calculated from the following equation:

$$S_A = 32.8 v^* \quad (5)$$

This 1-to-10 range of agitation intensity accounts for about 95%, or more, of all turbine-agitator applications, making it suitable for a wide range of process operations. Gates and his colleagues [5] provide guidelines on how to relate  $S_A$  to specific process applications.

The primary pumping capacity of an impeller is computed from the pumping number, the rotational speed and the impeller diameter:

$$Q_p = N_q N D^3 \quad (6)$$



Maximum allowed Z/T values						
$N_{Re}$ range	High-efficiency impeller		Four-bladed, 45-deg pitched impeller		Four-bladed flat or six-bladed impeller	
	Single	Dual	Single	Dual	Single	Dual
10 – 100	0.9	1.7	0.8	1.5	0.6	1.2
100 – 1,000	1.3	2.1	0.9	1.6	0.6	1.2
1,000 – 10,000	1.4	2.3	1.1	1.8	0.7	1.4
> 10,000	1.5	2.4	1.2	1.9	0.8	1.6

For single impellers:  $Z/6 \leq C \leq Z/2$ ; Standard  $C = Z/3$   
For dual impellers:  $Z/8 \leq C \leq 3Z/8$ ;  $Z/2 \leq C + S \leq 3Z/4$ ; Standard  $C = Z/3$ ,  $C + S = 2Z/3$

**TABLE 2.** The maximum allowed Z/T values vary, depending on whether the agitators have single or dual impellers

The characteristic velocity can be expressed as:

$$v^* \propto N_q N D \left( \frac{D^2}{T^2} \right) \quad (7)$$

This characteristic velocity scales geometrically and becomes

$$v^* \propto N_q N D \quad (8)$$

Therefore, during geometric scaleup, the characteristic velocity can be held constant by holding  $N_q N D$  constant.

High-efficiency impellers (Figure 1) of different sizes vary in their performance with respect to agitation intensity. One can use the pumping numbers from Figure 4 to estimate  $S_A$  for other such units.

For most turbine applications, replacing a pitched-blade impeller with a high-efficiency unit results in a significant improvement in the degree of agitation intensity. For example, a 1.5-kW agitator operating at a shaft speed of 0.75 rotations/s (45 rpm) in a 50-m<sup>3</sup> square-batch ( $Z/T = 1$ ) vessel equipped with a 1.558-m-dia. high-efficiency impeller provides  $S_A$  of just above 3 in a 1-Pa.s viscosity fluid. In contrast, a 1.154-m-dia. pitched-blade impeller in the same batch vessel draws the same power to produce  $S_A$  of just above 2.

#### Blending for material uniformity

The time required to achieve a certain degree of uniformity after a material is added to a tank is one of the most frequently specified process requirements. The uniformity of mixing is defined as:

$$U = 1 - \frac{[\Delta C(t)]_{\max}}{[\Delta C(0^+)]_{\max}} \quad (9)$$

Here  $\Delta C$  is the deviation from the average tank concentration, denoted by

$C_\infty$ . The uniformity usually increases according to an exponential function:

$$U(t) = 1 - e^{-k_m t} \quad (10)$$

where  $k_m$  is the mixing-rate constant. The above equation can be rearranged to yield an equation for the blend time required to achieve a certain degree of uniformity:

$$t_u = \frac{-\ln(1-U)}{k_m} \quad (11)$$

Mixing-rate constants		
Impeller style	$a$	$b$
Six-bladed disc	1.06	2.17
Four-bladed flat	1.01	2.30
Four-bladed 45-deg pitched	0.641	2.19
Three-bladed high-efficiency	0.272	1.67

**TABLE 3 (above).** The mixing-rate constants are for fully turbulent flow regimes ( $N_{Re} > 10,000$ )

**TABLE 4 (below).** The blend time for 99% uniformity with a pitched-blade turbine is about 50% longer than that with a high-efficiency impeller

Solution summary for Case Study 1		
	Three-bladed high-efficiency impeller	Pitched-blade impeller
$t_{99, \text{turb}}$ in s	114	171
$N_{Re}$	16,689	9,377
$f_{Re}$	1.00	1.00
$N_{Ri}$	2.08	3.70
$f_{\Delta p}$	2.65	2.50
$\mu^*$	50.0	50.0
$f_{\mu^*}$	1.06	1.13
$t_{99}$ in s	320	483

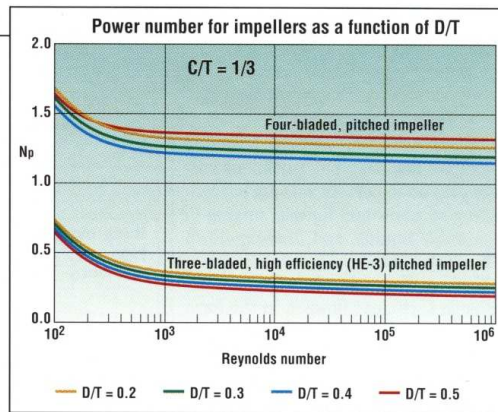


**FIGURE 3.** When called upon to load an agitator impeller to a given power level, one can use Equation 2 to calculate the required diameter of the impeller from the power number

For certain applications, such as acid-base neutralizations, it is desirable to predict the maximum and minimum concentrations at some time  $t$ . The following equations are obtained from rearrangements of the definition of the degree of mixing uniformity, and can be used to estimate the maximum and minimum concentrations at a specified time  $t$ .

$$\begin{aligned} C_{\min}(t) &= C_i + (C_\infty - C_i)U \\ C_{\max}(t) &= C_a - (C_a - C_\infty)U \end{aligned} \quad (12)$$

where  $C_{\min}(t)$  and  $C_{\max}(t)$  are the minimum and maximum concentrations anywhere in the tank at time  $t$ .  $C_i$  and  $C_\infty$  are the initial and final concentration of the added material in the bulk fluid, respectively.  $C_a$  refers to the concentration of the material added.

The dimensionless mixing-rate constant,  $k_m/N$ , in standard baffled tanks, is a function of impeller Reynolds number ( $N_{Re}$ ) and geometry. When  $N_{Re} > 10,000$ ,  $k_m/N$  is only a function of geometry, and is independent of  $N_{Re}$ . For fully turbulent conditions in standard baffled tanks,  $k_m$  can be determined experimentally from  $N$ ,  $D$ ,  $T$  and  $Z$  using the following relationship:

$$k_m = aN \left[ \frac{D}{T} \right]^b \left[ \frac{T}{Z} \right]^{0.5} \quad (13)$$

The constants  $a$  and  $b$  are provided in Table 3, as a function of impeller style in the turbulent range ( $N_{Re} > 10,000$ ).

Unless otherwise specified, blend times generally refer to the time required to achieve 99% uniformity and

can be calculated for turbulent conditions from the following equation:

$$t_{99} = \frac{4.605}{aN \left[ \frac{D}{T} \right]^b \left[ \frac{T}{Z} \right]^{0.5}} \quad (14)$$

Although  $a$  and  $b$  are for surface addition, blend times for similar fluids are relatively insensitive to addition location. Equation 14 is restricted to:

- Newtonian fluids of nearly the same viscosity and density as the bulk fluid
- Additions of 5%, or less, of the liquid volume of the vessel
- Additions made to a vessel already undergoing agitation. (Blend times of stratified fluids can be considerably longer)

One can account for the increased blend time at lower Reynolds number ( $100 < N_{Re} < 10,000$ ) and for the effects of fluids having different densities, using the following equation:

$$t_U = t_{U,turb} f_{Re} f_{\mu^*} f_{\Delta\rho} \quad (15)$$

The correction factor for lower Reynolds numbers is given in Figure 5.

Bouwman [6] identified three regimes of the effect of density difference and viscosity ratio on mixing time. The first is the impeller-controlled regime. The mixing time is impeller-controlled when the liquid is added near the impeller, or when the bulk flow succeeds in transporting the added fluid to the impeller. In this regime, the mixing time is practically independent of the viscosity ratio and the density difference. This has been verified for  $\mu^*$  up to 5,000, where  $\mu^*$  is defined as:

$$\mu^* = \frac{\mu_a}{\mu_o} \quad (16)$$

The second regime is controlled by gravity. The mixing time is gravity-controlled when materials of lower density than the bulk are added at the surface, or when lower-density materials added in the bulk rise to the surface and stay there. A similar situation occurs when a larger-density liquid added in the bulk sinks to the vessel bottom. The result is very long mixing times, which depend on the viscosity of both phases as well as on the density difference.

The third regime is marked by an intermediate behavior in which some portion of the added liquid is transported to the impeller and another part of the liquid either ends up at the liquid surface or sinks to the tank bottom. In this regime, there can be large variations in mixing time.

When minimal blend times are desired, the designer is advised to add the materials to be mixed as close to the

suction of the impeller as possible or introduce them directly into the impeller's vortex system. For the design of critical reactors involving competing or consecutive reactions, the recommendations of Fasano and Penney [7], and Tipnis and others [16] should be useful. When additions are made close to the impeller, so as to be immediately incorporated into the impeller's vortices, the blending is controlled by the impeller, and  $f_{\mu^*} = 1$  and  $f_{\Delta\rho} = 1$ . When this is not possible, and the materials are added at the surface approximate values of  $f_{\mu^*}$  and  $f_{\Delta\rho}$  can be determined.

Figure 6 shows  $f_{\mu^*}$  as a function of  $\mu^*$  and is based on data from Bouwman [6]. The data are based on a 45-deg, pitched-blade turbine at a 0.40 impeller- to tank-diameter ratio. Other impeller styles and different values of  $D/T$  are expected to produce somewhat different results. Until more definitive

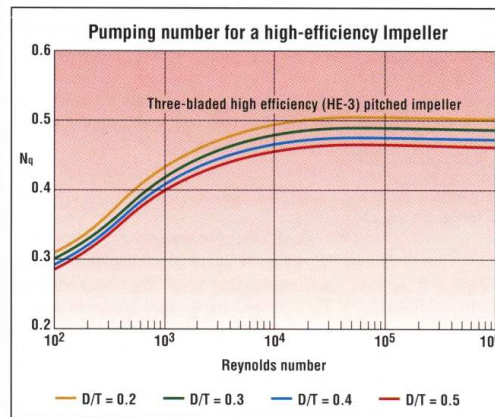
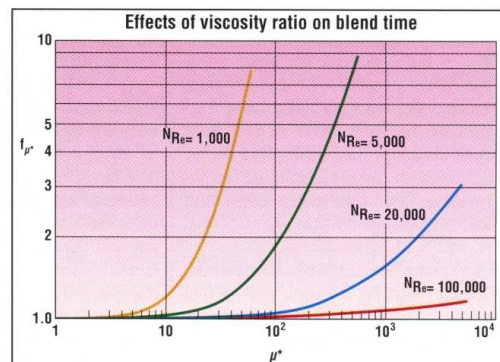
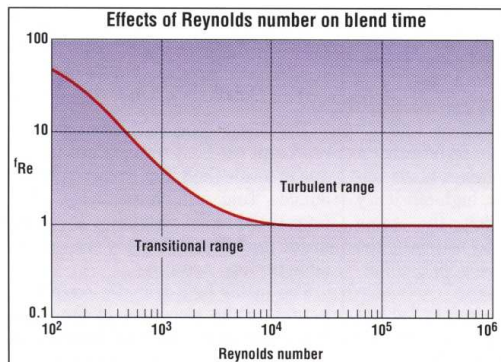


**FIGURE 4 (left).** Using Equations 5 and 8, one can estimate  $S_A$  from the pumping numbers for high-efficiency impellers

**FIGURE 5 (below left).** For  $N_{Re}$  values between 100 and 10,000,  $f_{Re}$  provides correction to the blend time for turbulent mixing

**FIGURE 6 (below right).** The  $f_{\mu^*}$  values provide estimates of the correction factor to blend time for viscosity differences





# ENGINEERING PRACTICE

Constants and corrections for heat transfer to tank wall		
Impeller style	K	Corrections, $f(T/Z, W/D)$
Six-bladed disc	0.74	$(T/Z)^{0.15}((W/D)/0.20)^{0.20}$
Four-bladed flat	0.66	$(T/Z)^{0.15}((W/D)/0.17)^{0.20}$
Four-bladed 45-deg pitched	0.45	$(T/Z)^{0.15}((W/D)/0.20)^{0.20}$
Three-bladed, high-efficiency (15)	0.31	$(T/Z)^{0.15}$

**TABLE 5.** The values of  $K$  and geometric corrections are for heat transfer to vessel walls of baffled tanks for  $N_{Re} > 100$

Constants and corrections for heat transfer to tank's dished bottom		
Impeller style	K	Corrections, $f(Z/T, W/D)$
Six-bladed disc	0.50	$((W/D)/0.20)^{0.20}$
Four-bladed flat	0.45	$((W/D)/0.17)^{0.20}$
Four-bladed, 45-deg pitched	1.08	$((W/D)/0.20)^{0.20}$
Three-bladed, high-efficiency	0.90	1

**TABLE 6.** The constant  $K$  and geometric corrections are for heat transfer to the dished bottom of baffled tanks for  $N_{Re} > 100$  and  $0.25 \leq C/T \leq 0.33$

data can be developed, Figure 6 serves as an approximate guide for estimating the effects of viscosity ratio.

Figure 7 shows  $f_p$  as a function of the Richardson number,  $N_{Ri}$ , which is a ratio of buoyancy to inertial forces:

$$N_{Ri} = \frac{\Delta \rho g Z}{\rho_o N^2 D^2} \quad (17)$$

$N_{Ri}$  is the primary correlating parameter when dealing with the effect of density differences on blend time. Figure 7 has been compiled from data from several sources, including Burmester [8]. However, these techniques for determining blend time have been found to be accurate only within about  $\pm 30\%$ .

## Blend time for multiple impellers

Often, an agitator is equipped with a number of impellers on the agitator shaft, and frequently these multiple impellers consist of different styles. The

number of variables that can influence blend time in such multiple-impeller systems increases dramatically. For example, the combination, order, orientation and relative pumping capacity of the impellers are only a few of the important factors that can affect blend time.

The blend time can be estimated from Equations 11 and 15 by substituting an effective mixing-rate constant

than that with the high-efficiency impeller.  $N_{Re}$  for the high-efficiency impeller is 44% higher than that for the pitched-blade turbine.

## Boosting heat transfer

The ability to remove or introduce heat into a vessel can be quite critical in reactive systems. Bulk temperatures higher or lower than the desired values

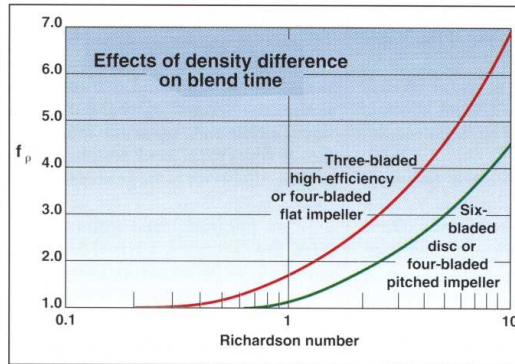


**FIGURE 7.** The Richardson number provides the primary correlating parameter in estimating the effect of density differences on blend time

( $k_{m,eff}$ ) for  $k_m$ .  $k_{m,eff}$  can be estimated by the sum of the individual mixing-rate constants ( $k_{m,i}$ ):

$$k_{m,eff} \approx \sum_{i=1}^n k_{m,i} \quad (18)$$

Each of the separate  $k_{m,i}$  should be based on a particular impeller operating separately with the total volume. This procedure is also accurate within about  $\pm 30\%$  in estimating blend times.

## Case Study 1

A 4-m-dia. tank with a flat bottom contains liquid to a depth of 4 m. The liquid in the tank has a viscosity of 100 mPa.s, and a density of 1,050 kg/m<sup>3</sup>. The material to be added has a viscosity of 5,000 mPa.s, and a density of 1,150 kg/m<sup>3</sup>. The tank can be fitted with an agitator rotating at 1.13 s<sup>-1</sup> (67.8 rpm). The agitator can be either a 0.889-m-dia., 45-deg pitched-blade impeller, or a 1.186-m-dia. high-efficiency impeller, both drawing the same power. The object is to estimate the time required to achieve a 99% uniformity for each impeller type.

The solution summarized in Table 4 reveals that the blend time with the pitched-blade turbine is 50% longer

than that with the high-efficiency impeller.  $N_{Re}$  for the high-efficiency impeller is 44% higher than that for the pitched-blade turbine.

can change product composition and physical properties. In addition, if the local heat-transfer coefficients vary widely from the mean, there can be hot or cold spots in a stirred reactor, which in turn can significantly alter product distribution or yield.

Dickey and Hicks [9] provide the basics for determining the rate of heat transfer in an agitated vessel:

$$q = U_i A_i (\theta_o - \theta_i) \quad (19)$$

The overall heat-transfer coefficient,  $U_i$ , neglecting fouling, can be calculated from the individual heat transfer resistances:

$$U_i = \frac{1}{\frac{1}{h_i} + \left( \frac{\Delta r}{k_w} \right) \left( \frac{A_i}{A_w} \right) + \left( \frac{1}{h_o} \right) \left( \frac{A_i}{A_o} \right)} \quad (20)$$

The three terms in the denominator represent the heat-transfer resistances due to inside fluid film, vessel wall, and outside fluid film, respectively. However, the thermal resistance due to the inside fluid film is the only one controllable through agitation.

The inside heat transfer coefficient,  $h_i$ , due to the resistance of the inside fluid film can be calculated from the following Nusselt number correlation:

Solution summary for Case Study 2		
	High- efficiency impeller	Four-blade pitched impeller
$N_{Pr}$	69,800	69,800
$N_{Re}$	885	495
Straight-side $\mu_w$ , Pa.s	0.472	0.470
Straight-side heat-transfer coeff., $W/m^2.K$	126	125
Bottom-head $\mu_w$ , Pa.s	0.816	0.720
Bottom-head heat-transfer coeff., $W/m^2.K$	340	282
Bottom-head surface area, $m^2$	14.2	14.2
Straight-side surface area, $m^2$	37.7	37.7
Total heat- transfer area, $m^2$	51.9	51.9
Overall heat-transfer coefficient, $W/m^2.K$	185	168

**TABLE 7.** The overall heat-transfer coefficient with a high-efficiency impeller is noticeably better than that with a pitched-blade impeller

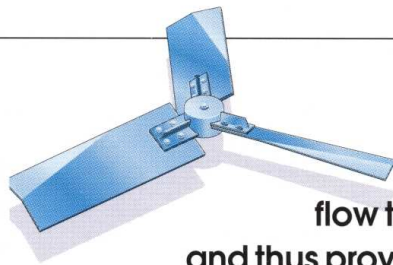
$$N_{Nu} = KN_{Re}^{\frac{2}{3}} N_{Pr}^{\frac{1}{3}} \left( \frac{\mu}{\mu_w} \right)^j f \left( \frac{T}{Z}, \frac{W}{D} \right) \quad (21)$$

where  $f(T/Z, W/D)$  represents various geometric correction factors. Existing data in the literature suggest that the exponents are 2/3 for the Reynolds number, 1/3 for the Prandtl number, and 0.14 for the viscosity ratio [10–13]. Therefore, essentially all impellers can be represented by:

$$N_{Nu} = KN_{Re}^{\frac{2}{3}} N_{Pr}^{\frac{1}{3}} \left( \frac{\mu}{\mu_w} \right)^{0.14} f \left( \frac{T}{Z}, \frac{W}{D} \right) \quad (22)$$

Table 5 provides the values for the constant,  $K$ , and the recommended geometric corrections for each of the most commonly used turbine-style impellers. Also included are the most recent data obtained with a high-efficiency impeller.

Fasano and others [14] have compared the local heat transfer characteristics of 6-bladed disc, 4-bladed 45-deg pitched, and high-efficiency impellers. It turns out that a high-efficiency impeller provides a more uniform profile for local heat-transfer coefficients at the tank wall. This is attributed to the



**A high-efficiency  
impeller produces  
a more-uniform  
flow throughout a vessel  
and thus provides a more-stable  
heat transfer profile at the vessel wall**

## NOMENCLATURE

$\alpha$	Constant in mixing-rate equation (Equation 13)	$k_{m,i}$	Mixing-rate constant for impeller $i$ , $s^{-1}$
$A_i$	Inside area of heat-transfer surface, $m^2$	$K$	Constant in Nusselt equation (Equation 21)
$A_o$	Outside area of heat-transfer surface, $m^2$	$n$	Number of impellers
$A_v$	Cross-sectional area of vessel, $m^2$	$N$	Impeller rotational speed, $s^{-1}$
$b$	Exponent in Equation 13	$N_{Fr}$	Froude number ( $=N^2 D/g$ )
$c$	Constant in Equation 21	$N_{Nu}$	Nusselt number ( $=h_i T/k$ )
$C$	Off-bottom clearance for the lowest impeller, m	$N_p$	Power number ( $=P/\rho N^3 D^5$ )
$C_a$	Concentration of material added, $kg/m^3$	$N_{Re}$	Reynolds number ( $=\rho N D^2/\mu$ )
$C_i$	Initial concentration, $kg/m^3$	$N_{Pr}$	Prandtl number ( $=C_p \mu/k$ )
$C(t)$	Time-dependent concentration, $kg/m^3$	$N_q$	Pumping number ( $=Q_p/N D^3$ )
$C_{min}(t)$	Minimum concentration in tank at time $t$ , $kg/m^3$	$N_{Ri}$	Richardson number ( $=\Delta \rho g Z/\rho_l N^2 D^2$ )
$C_{max}(t)$	Maximum concentration in tank at time $t$ , $kg/m^3$	$P$	Impeller power draw, W
$C_p$	Heat capacity, J/kg.K	$q$	Rate of heat transfer, W
$C_{\infty}$	Concentration at time $t = \infty$ , $kg/m^3$	$Q_p$	Primary pumping rate, $m^3/s$
$\Delta C(t)$	Concentration difference ( $=C(t) - C_{\infty}$ ) at time $t$ , $kg/m^3$	$\Delta r$	Wall thickness, m
$\Delta C(0^+)$	Initial concentration difference ( $=C(0^+) - C_{\infty}$ ), $kg/m^3$	$S$	Impeller scaling, m
$d$	Impeller diameter, m	$S_A$	Scale of agitation intensity
$D$	Constant in Equation 21	$t_U$	Blend time to uniformity $U$ , s
$f_{Re}$	Reynolds correction factor	$t_{U,turb}$	Time to blend to $U$ for $N_{Re} > 10,000$ , s
$f_{\Delta \rho}$	Density-difference correction factor	$t_{99}$	Time to achieve 99% uniformity, s
$f_{\mu^*}$	Viscosity-ratio correction factor	$T$	Vessel diameter, m
$g$	Acceleration due to gravity, $m/s^2$	$U$	Degree of uniformity, fraction (or % as subscript)
$h$	Off-bottom clearance for a probe, m	$U_i$	Overall heat-transfer coefficient, $W/m^2.K$
$h_i$	Inside (process side) heat-transfer coefficient at the wall, $W/m^2.K$	$V_{eq}$	Equivalent volume, gal
$h_o$	Outside heat-transfer coefficient at the wall, $W/m^2.K$	$v^*$	Characteristic velocity, $m/s$
$H$	Head, m	$W$	Blade width, m
$j$	Constant in Equation 21	$Z$	Liquid level in vessel, m
$k$	Thermal conductivity, J/m.s.K	$\Delta \rho$	Density difference ( $=\rho_a - \rho_0$ ), $kg/m^3$
$k_m$	Mixing-rate constant, $s^{-1}$	$\varepsilon$	Efficiency
$k_{m,eff}$	Mixing-rate constant for multiple-impeller system, $s^{-1}$	$\mu$	Viscosity, Pa.s
		$\mu_a$	Viscosity of material added, Pa.s
		$\mu_0$	Viscosity of vessel fluid before addition, Pa.s
		$\mu_w$	Viscosity at the tank wall, Pa.s
		$\mu^*$	$\mu_a/\mu_0$
		$\rho$	Density, $kg/m^3$
		$\rho_a$	Density of fluid added, $kg/m^3$
		$\rho_0$	Density of fluid in vessel before addition, $kg/m^3$
		$\theta$	Temperature, $^{\circ}C$
		$\theta_w$	Temperature at the wall, $^{\circ}C$
		$\tau$	Torque, N.m



more uniform flow generated by the high-efficiency impeller throughout the vessel.

Generally, when operated in the range  $0.25 \leq C/T \leq 0.33$ , axial-flow impellers, such as high-efficiency and pitched-blade impellers, generate dish-bottom heat-transfer coefficients at least twice the coefficients at the vessel's side wall. On the other hand, radial-flow impellers, such as Rushton turbines, reduce the heat transfer coefficients at the dish-head bottom by about 30%.

Therefore, when using axial-flow impellers, one is well-advised to jacket the dish bottom to facilitate heat transfer. Table 6 provides the values for the appropriate constants in Equation 21 for jacketed bottom-heads.

#### Case Study 2

A 4-m-dia. vessel contains a fluid to a level of 4 m. The bottom head is elliptically dished at 2:1 ratio of the major and minor axes. The fluid is to be heated through the straight-side and bottom-head jacket. The initial temperature of the fluid in the vessel is 20°C, while the jacket fluid temperature is 65°C. The thermal resistance due to the vessel wall and the jacket film have been estimated to be  $1.365 \times 10^{-3} \text{ m}^2 \cdot \text{K/W}$ . The thermal properties of the vessel fluid are as follows:  $C_p =$

$2.76 \times 10^{-3} \text{ J/kg} \cdot \text{K}$ ;  $k = 0.293 \text{ J/m} \cdot \text{s} \cdot \text{K}$ ; density =  $1,240 \text{ kg/m}^3$ . The viscosity at 20°C is 7.41 Pa.s, and the wall viscosity can be determined from the following equation:

$$\mu = 31.1 \exp(-0.0717\theta) \quad (23)$$

The agitator rotates at 1.67 rotations/s (100 rpm) and can be fitted with either a 1.78-m-dia. high-efficiency impeller or a 1.308-m-dia. pitched-blade impeller, both drawing the same power. The object is to determine the initial heat-transfer coefficient for each of these impellers.

The solution is summarized in Table 7. The overall inside heat-transfer coefficient for the high-efficiency impeller is 10% greater than that produced by the pitched-blade turbine. ■

Edited by Gulam Samdani

#### The authors

For biographical information on **Julian B. Fasano**, and **André Bakker**, refer to *CE*, January 1994, p. 100.

**W. Roy Penney** is a professor of chemical engineering at the University of Arkansas (Fayetteville). He has 25 years of experience in industrial process development and design with Phillips Petroleum, Monsanto, A. E. Staley, and Henkel Corp. He received his B.S. and M.S. degrees in mechanical engineering from the University of Arkansas, and Ph.D. in chemical engineering from Oklahoma State University.



#### References

1. Bakker, A., and others, Pinpoint Mixing Problems with Lasers and Simulation Software, *Chemical Engineering*, January 1994, pp. 94-100.
2. Bakker, A., and others, Computerizing the Steps of Mixer Selection, *Chemical Engineering*, March 1994, pp. 120-129.
3. Dickey, D. S., and Fenic, J. G., Dimensional Analysis for Fluid Agitation Systems, *Chemical Engineering*, January 5, 1976, pp. 139-145.
4. Hicks, R. W., and others, How to Design Agitators for Desired Process Response, *Chemical Engineering*, April 26, 1976, pp. 102-110.
5. Gates, L. E., and others, Application Guidelines for Turbine Agitators, *Chemical Engineering*, December 6, 1976, pp. 165-170.
6. Bouwmans, I., "The Blending of Liquids in Stirred Vessels," Ph.D. Thesis, Delft University of Technology, Netherlands, 1992.
7. Fasano, J. B. and Penney, W. R., Cut Reaction Byproducts by Proper Feed Blending, *Chemical Engineering Progress*, December 1991, pp. 46-52.
8. Burmester, S. S. H., and others, The Mixing of Miscible Liquids with Large Differences in Density and Viscosity, 7th European Conference on Mixing, 18-20 September 1991, Brugge, Belgium, pp. 9-16.
9. Dickey, D. S., and Hicks, R. W., Fundamentals of Agitation, *Chemical Engineering*, February 2, 1976, pp. 93-100.
10. Penney, W. R., Agitated Vessels (section 3.14); Heat Transfer Correlations (section 3.14.3), in "Heat Exchanger Design Handbook," (ed. by E. U. Schlunder), Hemisphere Publishing Corp., 1983.
11. Poggemann, R., and others, Heat Transfer in Agitated Vessels with Single-Phase Liquids, *German Chemical Engineering*, No. 3, 1980, pp. 163-174.
12. Uhl, V. W., Mechanically Aided Heat Transfer, in "Mixing Theory and Practice, vol. I, (ed. by Uhl V. W., and Gray, J. B.), Academic press, New York, 1966, pp. 279-328.
13. Nagata, S., "Mixing Principles and Applications," Halsted Press, 1975, pp. 85-119.
14. Fasano, J. B., and others, Local Wall Heat Transfer Coefficients Using Surface Calorimeters, Proc. 7th European Conference on Mixing, September 18-20, 1991, Brugge, Belgium, pp. 497-505.
15. Haam, S., and others, Local Heat Transfer in a Mixing Vessel Using a High-Efficiency Impeller, I&EC Research, 1993, 32, pp. 575-576.
16. Tipnis, S. K., and others, An Experimental Investigation to Determine a Scaled-up Method for Fast Competitive Parallel Reactions in Agitated Vessels, AIChE Symposium Series 299, Vol. 90, 1994, pp. 78-91.